Ceramics-Silikáty 66 (3), 374-383 (2022)
www.ceramics-silikaty.cz doi: 10.13168/cs.2022.0033

EFFECTS OF RAW MATERIAL RATIO, CURING TEMPERATURE AND MAGNESIUM OXIDE ACTIVITY ON THE HYDRATION OF BASIC MAGNESIUM SULFATE CEMENT

CHEN HONGDU*, NING XINKUANG* ,#WU CHENGYOU*,**

*School of Civil Engineering, Qinghai University, Xining 810016, PR China
**Key Laboratory of Energy-saving Building Materials and Engineering Safety of Qinghai Province , Xining 810016, PR China

#E-mail: wuchengyou86@163.com

Submitted June 4, 2022; accepted July 20, 2022

Keywords: Hydration, Microstructure, Hydration heat release, Temperature

The heat of hydration release rate and cumulative heat release of basic magnesium sulfate cement (BMSC) were determined by isothermal calorimetry. SEM and XRD were used to analyze the microstructure and phase composition of the hydration products of BMSC. The effects of raw material ratio, temperature, and MgO activity on the hydration exotherm, microstructure, and phase composition of basic magnesium sulfate cement were studied. The results showed that the ratio of raw materials affected the exothermic rate and phase composition of hydrated BMSC. Low-temperature curing led to the poor crystallinity of the strengthening phase in BMSC. Under high-temperature curing, BMSC hydration was more likely to generate $Mg(OH)_2$. The effect of magnesium oxide's activity on BMSC hydration was coupled with temperature, which influenceds the phase composition and the degree of crystallization of the strengthening phase.

INTRODUCTION

Basic magnesium sulfate cement (BMSC) is a magnesia cementitious material with $5MgSO_4 \cdot Mg(OH)_2 \cdot 7H_2O$ (5·1·7 phase) as the main hydration phase. It was developed after magnesium oxychloride cement and magnesium oxysulfate cement and is a magnesium oxysulfate cement modified by adding admixtures. BMSC has excellent properties such as its light weight, high strength, high toughness, and fire resistance, and it can be used in the production of decorative boards, fireproof boards, handicrafts, and thermal insulation materials [1-4].

The characteristics of cement itious materials are closely related to the type of hydration products, the relative content of hydration products, and the microstructure of cement. The mechanical properties of MOS cement depend mainly on the hydration history and the type and relative content of the hydration phase in hardened cement [5]. According to the ternary system of $MgO\text{-}MgSO_4\text{-}H_2O$, the following four primary phases can be found within the temperature range of 30 °C to 120 °C: a) $3Mg(OH)_2 \cdot MgSO_4 \cdot 8H_2O$ (3·1·8phase), b) $5Mg(OH)_2 \cdot MgSO_4 \cdot 3H_2O$ (5·1·3phase), c) $Mg(OH)_2 \cdot MgSO_4 \cdot 5H_2O$ (1·1·5phase) and d) $Mg(OH)_2 \cdot 2MgSO_4 \cdot 3H_2O$ (1·2·3 phase) [6].

Urwong et al. [7] investigated the formation of hydration phases in MOS cement and concluded that only the 3·1·8 phase is stable at ambient temperature. They also inferred that hardened MOS cement cannot be obtained when the content of the 3·1·8 phase exceeds the critical value of 50 %. This is due to the fact that the magnesium sulfate in this system cannot fully react with magnesium salts resulting in low strength values for MOS cement. In our previous work, after adding admixtures such as citric acid to MOS cement, it is beneficial to generate a large number of 5·1·7 phases, so that it has high strength and water resistance[8, 9]. Wu [1] named the modified magnesium oxysulfate cement as basic magnesium sulfate cement.

For magnesium cement, there are many factors that affect its performance. A et al. [10] studied the effect of magnesium hydroxide calcination and raw material ratio on the strength of magnesium oxychloride cement. The results showed that increasing the calcination temperature and molar ratio of active MgO to $MgCl_2$ increased the compressive strength of magnesium oxychloride cement specimens. Upon increasing the molar ratio of H_2O to $MgCl_2$, the compressive strength of the specimen decreased gradually. Ning et al. [11] studied the effects of curing temperature, the concentration of magnesium chloride solution, and the molar ratio of magnesium

oxide and magnesium chloride on the compressive strength of magnesium oxychloride cement. Ge et al. [12] studied the influence of ambient temperature and activity on the hydration and mechanical properties of magnesium oxychloride cement. Ye et al. [13] studied the effects of curing temperature and solution concentration on the structure and mechanical properties of magnesium oxychloride cement. The results indicated a close association between the curing temperature and phase structure and mechanical properties of magnesium oxychloride cement, and the molar ratio of H_2O:$MgCl_2$. The above-mentioned scholars studied the influence on macroscopic mechanical properties, and did not conduct detailed research on the influence mechanism. Miao [14] studied the effect and mechanism of different activated magnesium oxides on the performance of basic magnesium sulfate cement, but its research factors are too single. There are many factors involved in actual production, and it is difficult to consider only a single factor.

Based on the above reports, this study focused on the effects of raw material ratio, temperature, and MgO activity on the hydration of BMSC. When considering actual production, many factors may be involved. Therefore, this study not only considers a single factor but also considers the effect on BMSC hydration under the condition of multi-factor coupling. Studying the effects of the above factors on the hydration of BMSC can help predict the performance of BMSC and improve the actual production efficiency.

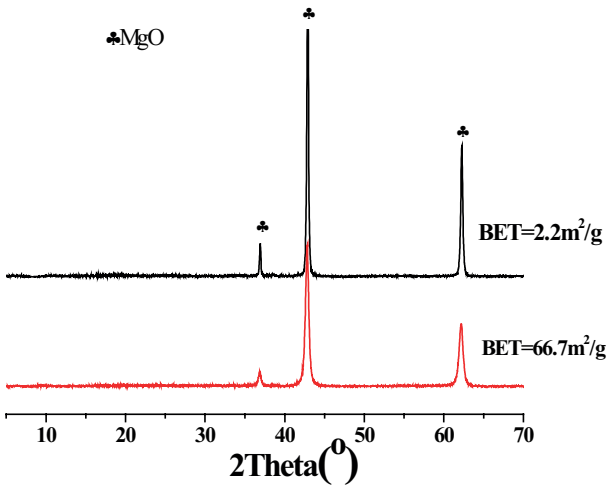

Figure 1. XRD patterns of the two kinds of MgO with different activities.

Table 1. Chemical composition of magnesium oxide B.

Composition	MgO	SiO_2	Al_2O_3	Fe_2O_3	CaO	I.L*
Wt. %	82.62	5.94	0.16	0.46	1.18	9.64

Annotation: I.L* is the weight loss at 1000 °C.

EXPERIMENTAL

Materials

The following are the materials that were used to prepare the test specimens.

(1) Magnesium oxide A: the specific surface area was 2.2 $m^2 \cdot g^{-1}$. It was locally produced in Qinghai Province, and its phase analysis is shown in Figure 1.

(2) Magnesium oxide B: the specific surface area was 14.0 $m^2 \cdot g^{-1}$. It was obtained by calcining magnesite at 750 - 900 °C (13820F-16520F) in Dashiqiao, Liaoning Province, China. The chemical composition is listed in Table 1.

(3) Magnesium oxide C: the specific surface area was 21.5 $m^2 \cdot g^{-1}$. Its phase analysis is presented in Figure 1. (analytical reagents; Shanghai Tongya Chemical Technology Development Co., Ltd.)

(4) Magnesium oxide D: the specific surface area was 66.7 $m^2 \cdot g^{-1}$. It was locally produced in Hebei Province, and its phase analysis is shown in Figure 1.

(5) Magnesium sulfate: magnesium sulfate heptahydrate [$MgSO_4 \cdot 7H_2O$] (analytical reagents; Tianjin Dingxin Chemical Co., Ltd.)

(6) Additives: analytical pure sodium citrate [$Na_3C_6H_5O_7 \cdot 2H_2O$] (Macleans Chemical Reagent Co., Ltd.) (CA was replaced in the follow-up paper).

The different active magnesium oxides used in the experiments are listed in Table 2.

Table 2. Different active magnesium oxide.

Types	A	B	C	D
specific surface area ($m^2 \cdot g^{-1}$)	2.2	14.0	21.5	66.7

Preparation of the BMSC sample

MgO samples with different specific surface areas were selected depending on the experimental purpose. Sodium citrate comprised 5 % of the MgO mass. $MgSO_4 \cdot 7H_2O$ was dissolved in water to form a 25 % magnesium sulfate solution, and a heat of hydration experiment was conducted following instructions specific to the apparatus, with a molar ratio M (MgO:$MgSO_4$:H_2O) = = n:1:20 (n = 5, 6, 7, 8). According to the above molar ratio, MgO and $MgSO_4$ solution and sodium citrate were stirred to form the slurry and then poured into a rigid mold of 20 mm × 20 mm × 20 mm. The film was released after curing for 24 h and then maintained at the temperature required for the experiment.

For convenience, the following labels are used: "XMmTt" denotes different BMSC cement products, where "X" represents the type of MgO used in the experiment, "m" is the molar ratio of MgO/$MgSO_4$, and "T" indicates the curing temperature of the BMSC sample. For example, AM5T10 represents a sample prepared using MgO with a specific surface area of 2.2 $m^2 \cdot g^{-1}$, the molar ratio of MgO/$MgSO_4$ of 5, and a curing temperature of 10 °C.

Sample analysis

After grinding the BMSC cement samples to D90 < 74 μm, its phase composition was tested by a DT300 X-ray diffractometer (voltage = 40 kV; current = 30 mA), and Topas4.2 software was used to fit the XRD patterns for quantitative analysis. A JSM-6610LV scanning electron microscope was used to analyze the micro-morphology of the samples. A Calmetrix-4000HPC isothermal microcalorimeter was used to measure the exothermic hydration of the samples. All BMSC hydration exothermic curves in the experiment were based on the mass of MgO in the BMSC raw material.

RESULTS AND DISCUSSION

Effect of raw material ratio on BMSC hydration

BMSC is composed of MgO, hydrated $MgSO_4$, admixtures, and water in a certain proportion [15]. MgO and hydrated $MgSO_4$ are important raw materials of BMSC, and it is important to study the effect of their ratio on the hydration of BMSC.

Figures 2 and 3 present the hydration exothermic rate curve and the cumulative exothermic curve of CMmT20 (m = 5, 6, 7, 8). Figure 4 presents the XRD pattern after hydration for 7 d. Wu (2014) divided BMSC hydration into the induction prophase, induction phase, acceleration phase, deceleration phase, and stable phase. Based on the aforementioned divisions, the times required for the hydrated sample to enter the acceleration phase were 3.8, 5.3, 8.8, and 8.3 h in the order of the molar ratio from large to small. CM8T20 and CM7T20 entered the acceleration phase earlier than CM6T20 and CM5T20. It can be seen that the larger the molar ratio, the earlier hydration entered the acceleration phase. The reason is that the larger the molar ratio, the easier it is for the ions dissolved in the cement slurry per unit mass to reach the supersaturation of 5·1·7 phase precipitation after MgO hydration. Compared with CM6T20, CM5T20 entered the acceleration stage earlier, mainly because the paste consistency between CM6T20 and CM6T20 varied only slightly. Moreover, compared with CM6T20, CM5T20 had a sufficient $MgSO_4$ content and, thus, more easily reached supersaturation of the 5·1·7 precipitated phase. It can be seen from the cumulative heat release curve in Figure 3 that during the monitoring time, the cumulative heat release of CM5T20 and CM6T20 was higher than that of CM7T20. The reason is that in the cement slurry per unit mass, the proportion of cement raw materials in CM5T20 and CM6T20 was closer to the formation ratio of 5·1·7 phase than in CM7T20, which was more conducive to the formation of 5·1·7 phase in the later stage of hydration. CM8T20 showed the highest accumulated heat of hydration, which was attributed to its high MgO content and the lack of $MgSO_4$ in the later stages of hydration. This led to the formation

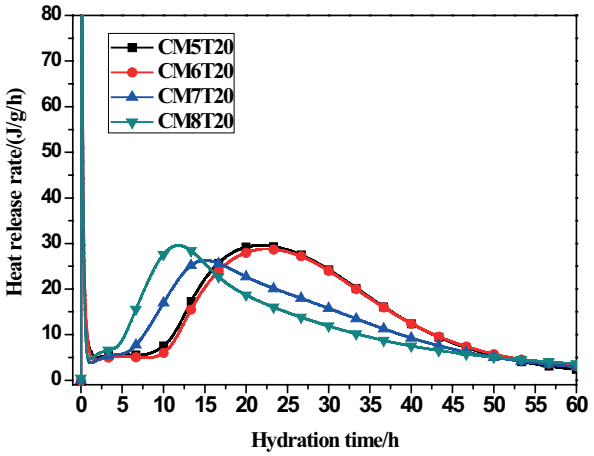

Figure 2. Heat of hydration release rate curve for the BMSC samples with different molar ratios.

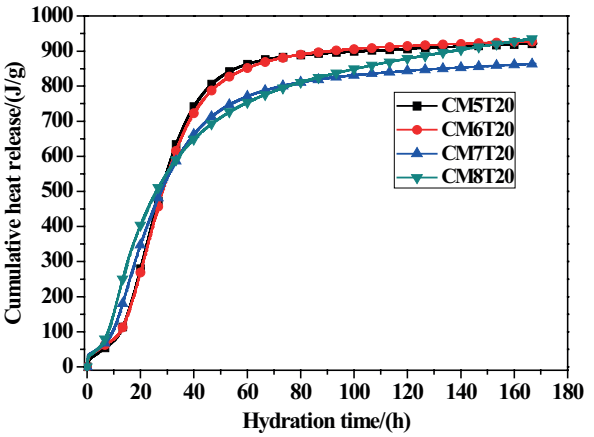

Figure 3. Cumulative heat of hydration release curve for the BMSC samples with different mole ratios.

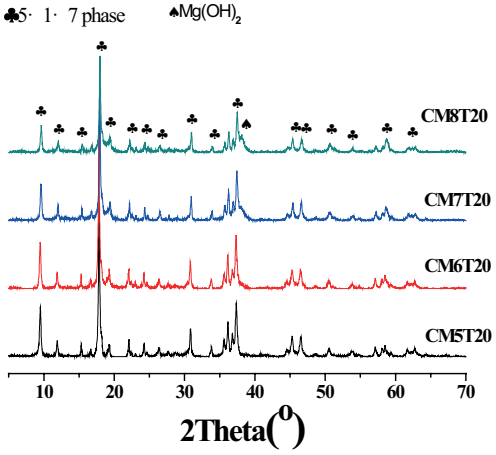

Figure 4. XRD patterns of the BMSC samples with different mole ratios after curing for 7 d.

of a large amount of $Mg(OH)_2$. Based on the XRD pattern in Figure 4, upon increasing the molar ratio, the intensity of the 5·1·7 phase diffraction peak decreased, and the intensity of the $Mg(OH)_2$ peak increased. This observation indicates that the higher the molar ratio, the less 5·1·7 phase was present in BMSC hydration

products, and the greater the amount of $Mg(OH)_2$. The aforementioned analysis was further verified.

The higher the $MgO:MgSO_4$ mole ratio, the shorter the induction period. The molar ratio also affected the composition of the hydrate phase. For BMSC prepared with a high $MgO:MgSO_4$ molar ratio using MgO with a specific surface area of 21.5 $m^2 \cdot g^{-1}$, a large amount of $Mg(OH)_2$ was generated later, which led to lower strength and poor crack resistance. However, for MgO with a small specific surface area, the strength development law varied, hence the correlation between BMSC hydration and MgO activity. Therefore, for the actual production of BMSC prepared with MgO with a specific surface area of 21.5 $m^2 \cdot g^{-1}$, the high molar ratio early strength developed faster, but the late strength was low. The low molar ratio had a low early strength and high late strength. By considering the production efficiency and product quality, a low $MgO:MgSO_4$ mole ratio decreased the consumption of MgO raw materials and reduced the production costs; however, the early-strength development was slow, and the production efficiency was relatively low. The opposite is true for the preparation of BMSCs at high $MgO:MgSO_4$ molar ratios. Therefore, the raw material ratio of BMSC should be considered according to the actual production situation.

Effect of temperature on BMSC hydration

For the hydration of cementitious materials, the curing temperature must be considered because it can markedly affect the hydration reaction, and, consequently, the BMSC performance.

Figure 5 and 6 present the curves for the heat of hydration release rate and the accumulated heat of hydration release of the BMSC samples − CM5T10, CM5T20, and CM5T30. As determined from the heat of hydration release rate in Figure 5, the hydration induction time of CM5T10 was about 33.6 h, and the hydration induction time of CM5T20 was about 7.25 h − that is, 78.42 % shorter than that of CM5T10. The hydration time of CM5T30 was about 4.5 h − that is, 86.6 % shorter than that of CM5T10. It can be seen that upon increasing the curing temperature, the BMSC induction period was shortened because, as the temperature decreases, the chemical reaction rate decreases, and the dissolution rate of MgO in the early stage becomes slower. When the temperature was increased, the induction period of CM5T30 was shortened by 37.9 % compared with that of CM5T20. When the temperature was lowered, the induction period of CM5T10 was prolonged by 363.4 % compared with that of CM5T20.The induction period of the hydration reaction in BMSC was more affected by lower temperatures. As shown in Figure 5, the higher the temperature, the steeper the second exothermic peak of the heat of hydration release rate curve, and the larger the peak value. The steeper the peak, the larger the peak value, indicating that the hydration reaction in cement was more intense during this period. Thus, the lower the temperature, the milder the hydration. It can be seen from the cumulative heat release curve in Figure 6 that the higher the temperature, the greater the early cumulative heat release. This corresponds to the phenomenon that the higher the temperature, the shorter the induction period, as shown by the hydration exothermic rate curve in Figure 5. As shown in Figure 6, CM5T10 exhibited the largest heat release, and CM5T20 only slightly varied from CM5T30. The main reason may be that for this active MgO, since the curing temperature of CM5T20 and CM5T30 were similar, it had little effect on the phase composition of BMSC.

Figure 7 shows the XRD patterns of BMSC after curing at different temperatures for 1 d, where the specific surface area of MgO used to prepare BMSC

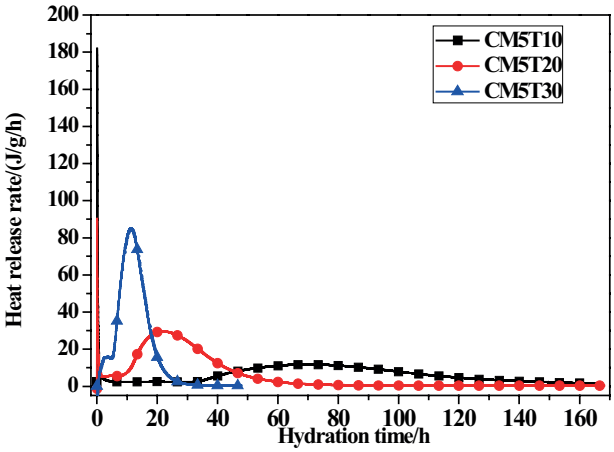

Figure 5. Heat of hydration release rate curves for the BMSC samples at different temperatures.

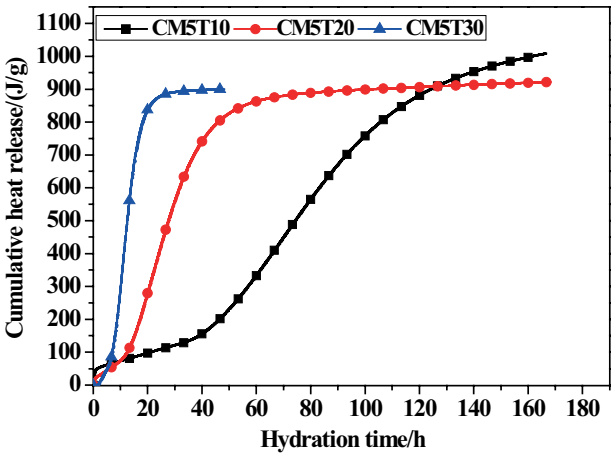

Figure 6. Cumulative heat of hydration release curve for the BMSC samples at different temperatures.

was 21.5 $m^2 \cdot g^{-1}$. It can be seen from Figure 7 that upon increasing the curing temperature, the diffraction peak intensity of MgO became smaller, showing that the higher the curing temperature, the lower the MgO content in the samples. The primary reason is that the higher the temperature, the faster the hydration of

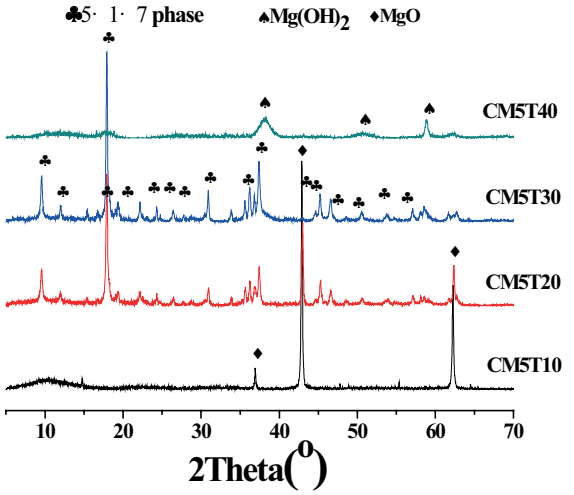

Figure 7. XRD patterns of the BMSC samples cured at different temperatures for 1 d.

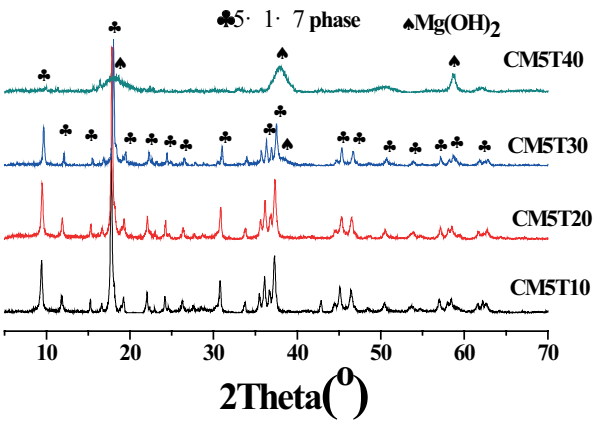

Figure 8. XRD patterns of the BMSC samples cured at different temperatures for 7 d.

MgO, which corresponds to the rule in Figure 5. This indicates that the higher the temperature, the shorter the induction period. The curing temperature also influenced the degree of crystallization of BMSC. The SEM of the sample cured for 1 d is presented in Figure 8, which reveals that the whisker of the CM5T10 and CM5T20 samples was markedly smaller than that of CM5T20. This was mainly related to the supersaturation of crystal precipitates. When the temperature is lower, the supersaturation of crystal precipitates is higher, and the nucleation rate is faster, resulting in a smaller crystal size. In addition, the curing temperature also affected the phase composition of BMSC hydration. Figure 9 shows the XRD patterns of the BMSC specimens after curing at different temperatures for 7 d, where the BET of MgO used to prepare BMSC was 21.5 $m^2 \cdot g^{-1}$. The intensity of the 5·1·7 phase in CM5T40 and CM5T30 was markedly lower than that in CM5T20 and CM5T10. There were $Mg(OH)_2$ peaks in the XRD patterns of CM5T40 and CM5T30. As shown in Figure 7, the temperature led to a phase change in the BMSC during hydration due to the different activation energies between the 5·1·7 phase and $Mg(OH)_2$. As a result, BMSC was more likely to form the 5·1·7 phase when cured at low temperatures, and $Mg(OH)_2$ was more likely to form when cured at high temperatures.

Temperature affects the BMSC hydration process. When the curing temperature was lower, the hydration induction period of BMSC was longer, and the hydration reaction proceeded more gently. At the same time, the curing temperature affected the phases in BMSC after hydration. When the curing temperature was higher, although the hydration rate was faster, the hydration of BMSC was more likely to generate $Mg(OH)_2$, which is not conducive to improving the strength of BMSC. In addition, the curing temperature also affected the crystallization degree of BMSC. Under low-temperature curing, the crystal size was smaller than that at normal

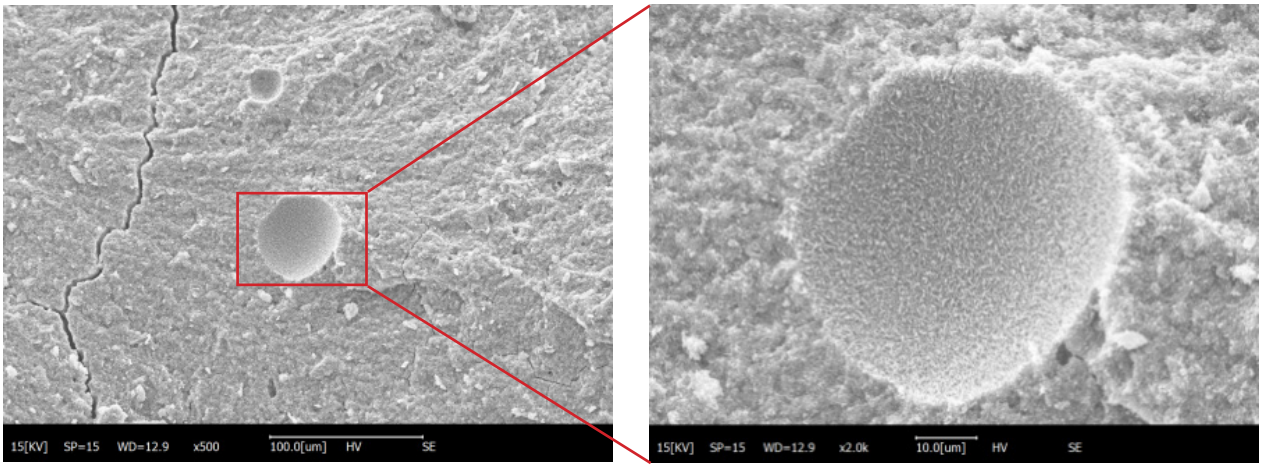

a) CM5T10 × 500 b) CM5T10 × 2000

Figure 9. SEM images of the BMSC samples cured at different temperatures for 7 d.

(*Continue on next page*)

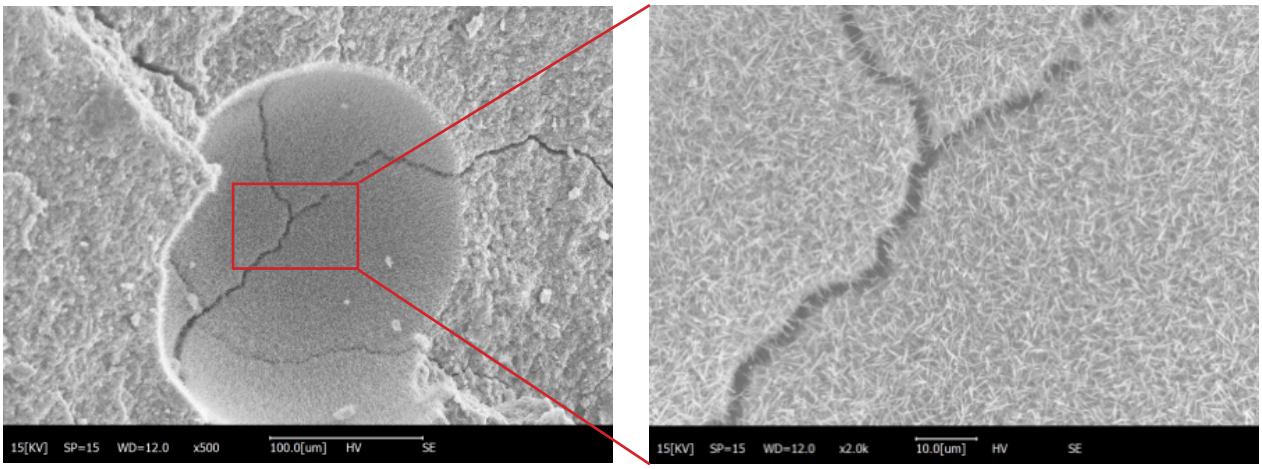

c) CM5T20 × 500 d) CM5T20 × 2000

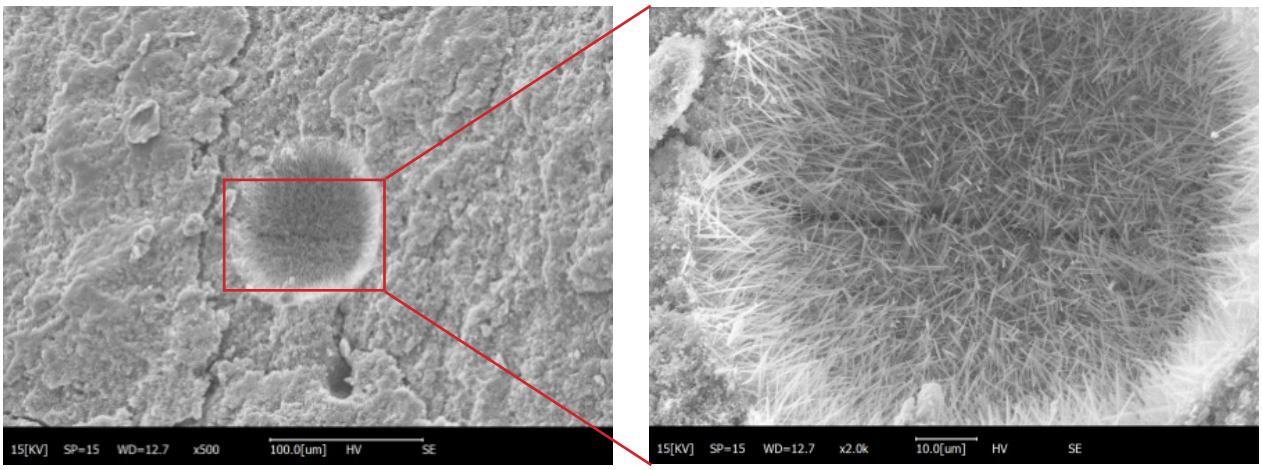

e) CM5T30 × 500 f) CM5T30 × 2000

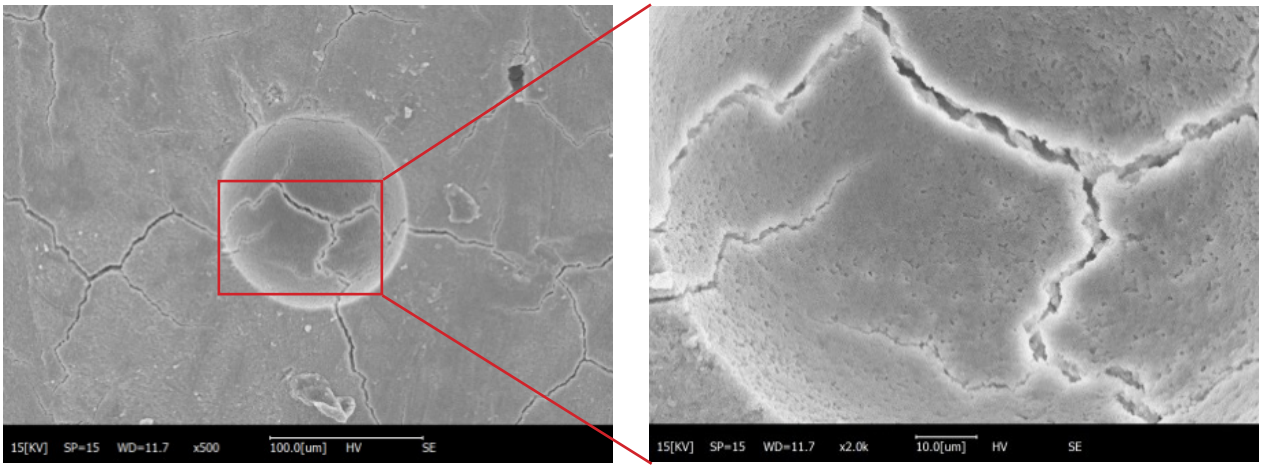

g) CM5T40 × 500 h) CM5T40 × 2000

Figure 9. SEM images of the BMSC samples cured at different temperatures for 7 d.

temperature. Therefore, during actual production, BMSC specimens should not be cured at a high temperature, which leads to a low strength in the later stage. If the temperature is too low, the development of strength in the earlier stage will be slow, which is not conducive to improving the production efficiency.

Effect of MgO activity on BMSC hydration

The activity of MgO activity markedly affects the hydration rate and mechanical properties of BMSC. However, during actual production, many factors need to be considered, including magnesium oxide activity, temperature, and other factors. MgO activity varies

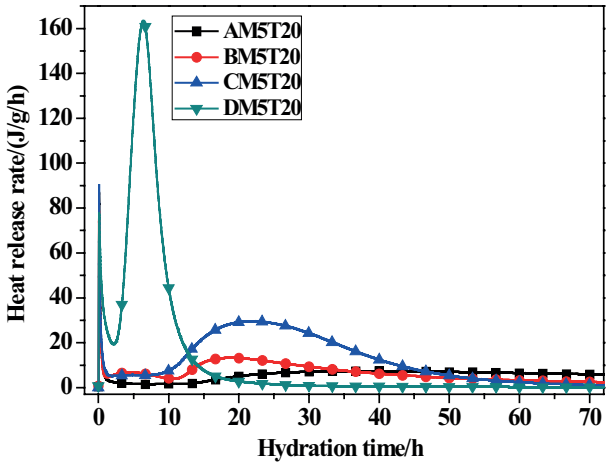

Figure 10. Heat of hydration release rate curves for BMSC prepared with different MgO activities .

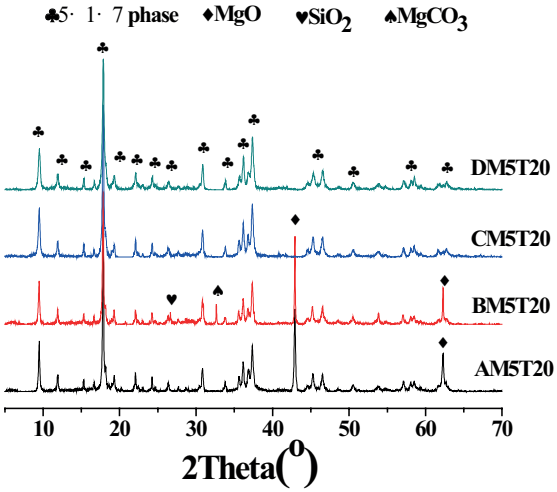

Figure 11. XRD patterns of BMSC with different MgO activities after hydrating for 7 d.

with its specific surface area. Therefore, the effects of the coupling between activity, activity and temperature, activity and molar ratio on BMSC hydration were studied.

BMSC samples were prepared by using MgO with specific surface areas of 2.2 $m^2 \cdot g^{-1}$, 14.0 $m^2 \cdot g^{-1}$, 21.5 $m^2 \cdot g^{-1}$, and 66.7 $m^2 \cdot g^{-1}$, respectively. The heat of hydration of BMSC was determined at 20 °C to evaluate the effect of activity on the heat of hydration of BMSC. Figure 11 is the XRD pattern of the BMSC sample hydrated for 7 d. As shown in Figure 10, the induction period of BMSC was extended with a decrease in MgO activity, which was attributed to the lower activity and slower hydration of MgO. Moreover, the maximum exothermic peak decreased with a reduction in the MgO activity. It shows that the lower the activity of MgO, the more mild the hydration reaction of BMSC is when it enters the accelerated phase. Figure 11 shows a peak of unreacted MgO in BM5T20 and AM5T20, which confirms that the lower the activity, the slower the hydration reaction.

In addition, the MgO activity influences the crystallization degree of BMSC. Figure 10 presents SEM images of BM5T20 and DM5T20 after reacting for 7 d. As observed, the lower the activity, the higher the degree of crystallization of the 5·1·7 phase, and the larger the grain size. At the same time, we can also verify from the peak width of the main peak of the 5·1·7 phase in Figure 9 that the lower the activity of MgO, the sharper the diffraction peak of the 5·1·7 phase. This indicates a larger grain size.

For BMSC prepared with a high MgO:$MgSO_4$ molar ratio, the effect of MgO activity on the hydration process of BMSC was different from that of a low MgO:$MgSO_4$ molar ratio. Figure 13 shows the hydration exothermic rate curves of BMSC obtained under curing at 20 °C with different active magnesium oxides, a MgO:$MgSO_4$:H_2O molar ratio of 8:1:20, and sodium citrate added was 0.5 % of the mass of MgO. When the activity of MgO was higher, the hydration induction period of BMSC was shorter, and the hydration reaction was more intense in

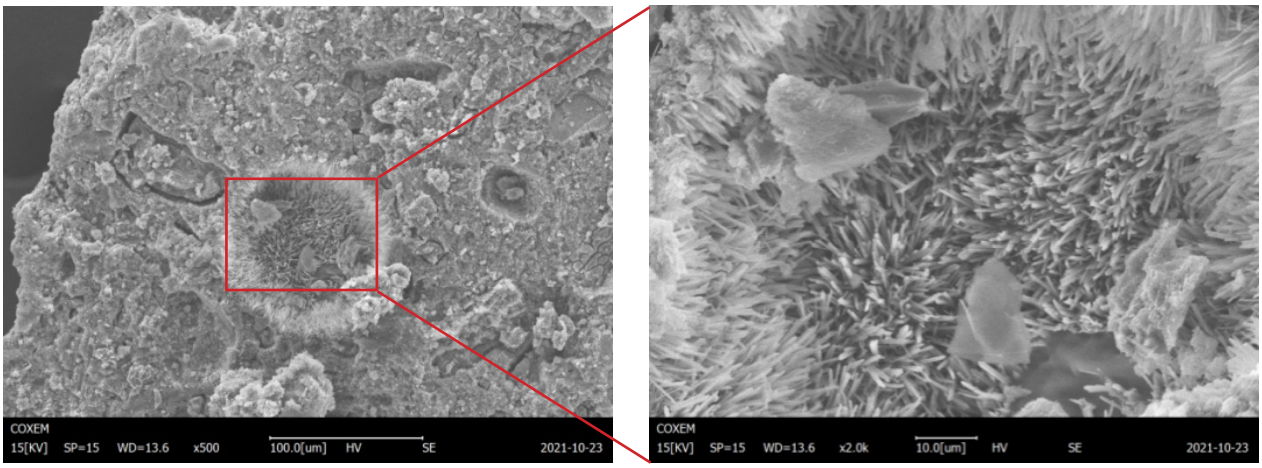

a) BM5T20 × 500 b) BM5T20 × 2000

Figure 12. SEM images of BMSC with different MgO activities after being hydrated for 7 d.

(*Continue on next page*)

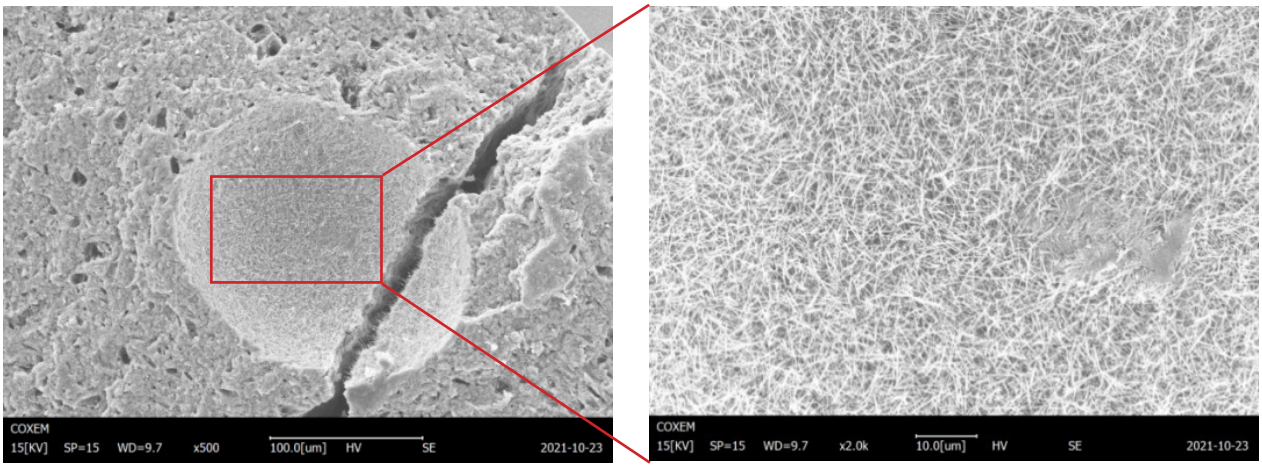

c) DM5T20 × 500 d) DM5T20 × 2000

Figure 12. SEM images of BMSC with different MgO activities after being hydrated for 7 d.

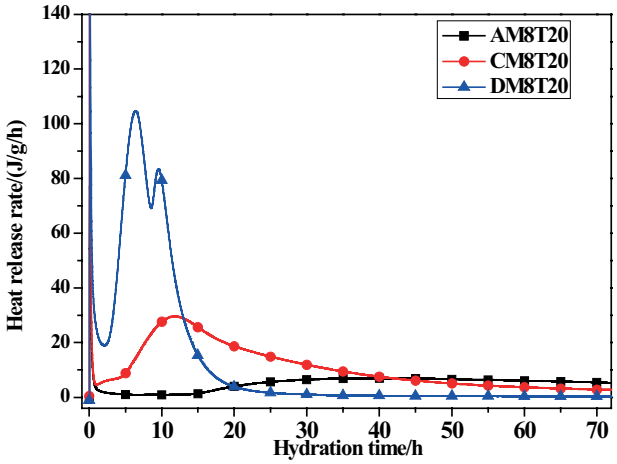

Figure 13. Heat of hydration release rate curves of BMSC samples prepared with different MgO activities.

the accelerated phase. This was consistent with the above rules. However, the exothermic hydration rate curves for the BMSC samples prepared with different MgO activity

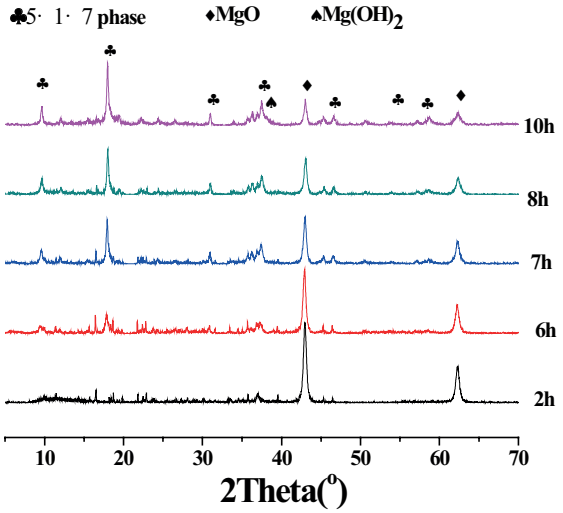

Figure 14. DM8T20 early-phase tracing XRD patterns.

levels were markedly different. A third exothermic peak appeared in specimen DM8T20. Figure 14 presents the phase tracking of DM8T20 with a molar ratio of 8. A new $Mg(OH)_2$ phase appeared at 10 h, and a third exothermic peak appeared in DM8T20 about 10 h after hydration. Therefore, when using MgO with a specific surface area of 66.7 $m^2 \cdot g^{-1}$ to prepare BMSC specimens, the third heat release peak appeared in the hydration heat release rate curve because $Mg(OH)_2$ phase was generated during the hydration reaction.

Moreover, the effect of activity on the hydration of BMSC cured at high temperatures differed from that cured at a normal temperature. As determined from the hydration exothermic rate curves of DM5T30 and CM5T30 in Figure 15, the effect of activity on the hydration law was consistent with the aforementioned law under normal-temperature curing in Figure 10. However, under high-temperature curing, the hydration products of the BMSCs were different. Figure 16 presents the XRD patterns of DM5T30 and CM5T30 specimens

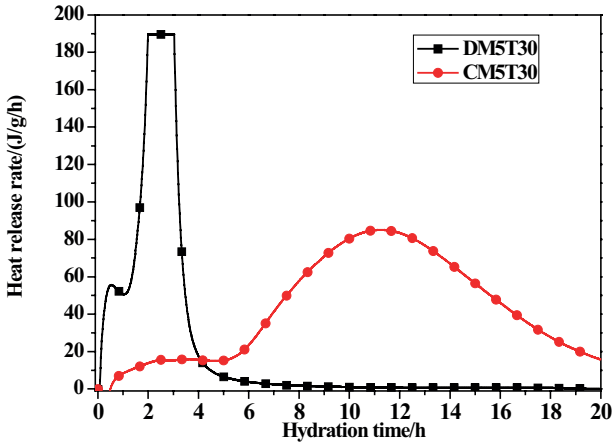

Figure 15. Heat of hydration release rate curves for BMSC samples prepared with different MgO activities.

cured for 3 d. As shown in the figure, the main hydrate of CM5T30 was the 5·1·7 phase, whereas that of DM5T30 was $Mg(OH)_2$ and the unreacted hydrate $MgSO_4$. In Figure 11, the main hydration product of DM5T20 was the 5·1·7 phase at room temperature. It can be seen that when BMSC specimens were prepared with different active MgO, the required curing temperature was different. To obtain BMSC with better properties, BMSC prepared from MgO with a lower activity could withstand higher curing temperatures than those with a higher activity.

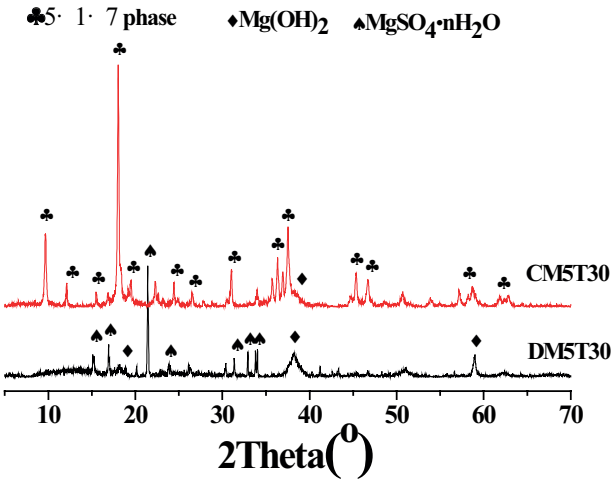

Figure 16. XRD patterns of BMSC hydration 3d.

When the activity of MgO was higher, the induction period of BMSC hydration was shorter. To prepare BMSC specimens using the more active MgO, when the molar ratio was high, a third exothermic peak appeared in the hydration exothermic rate curve. The activity of MgO also affected the crystallinity of the 5·1·7 phase in BMSC. In addition, the temperature required for curing of BMSCs prepared from different active MgO was also different. BMSC prepared from MgO with a lower activity could withstand a higher curing temperature than MgO with a higher activity.

CONCLUSIONS

In this study, the effects of the raw material ratio, temperature, and activity on the hydration process, micromorphology, and phase composition of basic magnesium sulfate cement were evaluated. The following conclusions were drawn:

(1) The ratio of raw materials affected the hydration of BMSC. When the $MgO:MgSO_4$ molar ratio was higher, the hydration induction period was shorter. Simultaneously, the molar ratio of $MgO:MgSO_4$ also affected the composition of the hydrated phases in BMSC. BMSC prepared with a high molar ratio of $MgO:MgSO_4$ was more likely to generate $Mg(OH)_2$ during hydration.

(2) Temperature affected the hydration of BMSC. When the temperature was relatively low, the hydration reaction of BMSC was milder, and the hydration induction period of BMSC was longer. At the same time, the temperature changed the hydrated phase of BMSC.

(3) Although the hydration rate of BMSC was accelerated under higher-temperature curing, it was more likely to generate $Mg(OH)_2$, which was not conducive to improving the strength of BMSC.

(4) The curing temperature also affected the crystallization degree of BMSC. The crystal size was smaller under low-temperature curing than under normal-temperature curing.

(5) The activity of MgO affected the hydration process of BMSC. When the activity of MgO was higher, the induction period of BMSCs was shorter. When BMSC was prepared from more active MgO, when the molar ratio of $MgO:MgSO_4$ was high, a third exothermic peak appeared. In addition, the activity also affected the crystallinity of the 5·1·7 phase in BMSC.

(6) The temperature required for the curing of BMSC prepared from MgO with different activities was different. BMSC prepared from MgO with a lower activity could withstand a higher curing temperature than MgO with a higher activity.

Acknowledgement

This study was supported by the National Natural Science Foundation of China (grant no. 52002202 and 51662035), the Applied Fundamental Research Project of Qinghai Province (grant no. 2019-ZJ-7005), and the West Light Project of the Chinese Academy of Sciences.

REFERENCES

1. Chengyou W. (2014). *Fundamental theory and civil engineering application of basic magnesium sulfate cement.* The University of Chinese Academy of Sciences.
2. Sainan X., Chengyou W., Hongfa Y. (2018): Accelerated Aging Test and Microscopic Mechanism of Glass Fiber Reinforced Basic Magnesium Sulfate Cement. *Bulletin of the Chinese Ceramic Society, 37*(2), 411-416. doi:10.16552/j.cnki.issn1001-1625.2018.02.006
3. Chengyou W., Huifang Z., Hongfa Y. (2012): Extraction of aluminium from fly ash by pressurized acid leaching. *Transactions of Nonferrous Metals Society of China, 22*(09), 2282-2288.
4. Chengyou W., Wenhai C., Huifang Z. (2017): The hydration mechanism and performance of Modified magnesium oxysulfate cement by tartaric acid. *Construction and Building Materials, 144*, 516-524. doi: 10.1016/j.conbuildma t. 2017.03.222
5. Chengyou W., Cong C., Huifang Z., Yongshan T., Hongfa Y.(2018): Preparation of magnesium oxysulfate cement

using magnesium-rich byproducts from the production of lithium carbonate from salt lakes. *Construction and Building Materials, 172,* 597-607. doi: 10.1016/j.conbuildmat.2018.04.005.

6. Demediuk, T., Cole, W. F. (1957): A study of magnesium oxysulfates. *Australian Journal of Chemistry, 10*(3), 287-294. Doi: 10.1071/CH9570287
7. Urwong L., Sorrell C. A., (1980): Phase relations in magnesium oxysulfate cements. *Journal of the American Ceramic Society, 63*(9-10),523-526. Doi: 10.1111/j.1151-2916.1980.tb10757.x
8. Chengyou W., Hongfa Y., Jingmei D., Lina Z. (2014): Effects of material ratio, fly ash, and citric acid on magnesium oxysulfate cement. *Materials Journal, 111*(3), 291–297. doi: 10.14359/51686723
9. Chengyou W., Hongfa Y., Huifang Z., Jinmei D., Jing W., Yongshan T.(2015): Effects of phosphoric acid and phosphates on magnesium oxysulfate cement. *Materials and structures, 48*(4) ,907–917. doi: 10.1617/s11527-013-0202-6
10. Danchun A., Xueying X., Jing W., Jinmei D., Weixin Z.,Chenggong C., Pan L., Fei D., Qin H. (2020): Effect of Magnesium hydroxide process and raw material ratio on compressive strength of magnesium oxychloride cement. *Salt Lake studies, 28*(03), 85-92.
11. Yayu N., Lengqing Z., Xiangqun D. (2016): Influence of some factors on the properties of magnesium oxychloride cement. *Silicate bulletin, 35*(07), 2287-2290. doi:10.16552/j.cnki.issn1001-1625.2016.07.053
12. Shaojin G., Xu Z., Hongyu W., Ruoyu C. (2019): Effect of high activity MgO on phase and properties of magnesium oxychloride cement at low temperature. *Journal of silicates, 47* (07), 865-873. doi:10.14062/j.issn.0454-5648.2019.07.0 2
13. Qianqian Y., Wen W., Wei Z., Jianzhang L., Hui C. (2018):Tuning the phase structure and mechanical performance of magnesium oxychloride cements by curing temperature and $H_2O/MgCl_2$ ratio. *Construction and Building Materials, 179,* 413-419. doi:10.1016/j.conbuildmat.2018.05.257
14. Meng M. (2021): Effect of different active MgO on performance and mechanism research of basic magnesium sulfate cement. Qinghai University. doi:10.27740/d.cnki.gqhdx.2021.000353
15. Tao G., Hefang W., Hongjian Y., Xiaosen C., Qiu M., Shaoming Y. (2017): The mechanical properties of magnesium oxysulfate cement enhanced with 517 phase magnesium oxysulfate whiskers. *Construction and Building Materials, 150*, 844–850. doi:10.1016/j.conbuildmat.2017.06.024